An Automated Nowcasting Model of Significant Instability Events in the Flight Terminal Area of Rio de Janeiro - Brazil

Gutemberg Borges França*, Manoel Valdonel de Almeida, and Alessana C. Rosette,

Federal University of Rio de Janeiro (UFRJ), Rio de Janeiro, Brazil

*E-mail address: gutemberg@lma.ufrj.br; Tel.: +55 (21) 2598-9523

Abstract

This paper presents an alternative automated model, based on neural network techniques, to produce short-term and locally specific forecasts of significant instability for flight in the terminal area of Rio de Janeiro, Brazil. Twelve years of data were used for neural network training/testing and validation. Data are originally from four sources: 1) hourly meteorological observations from surface meteorological stations at five airports distributed around the study area; 2) atmospheric profiles collected twice a day at the meteorological station at Galeão Airport; 3) rain rate data collected from a network of twenty-nine rain gauges in the study area; and 4) lightning data regularly collected by national detection networks. An investigation was undertaken regarding the capability of a neural network to produce early warning signs—or as a nowcasting tool—for significant instability events in the study area. The automated nowcasting model was validated using results from five categorical statistics, indicated in parentheses in forecasts of the first, second, and third hours, respectively—namely: proportion correct (0.99, 0.97, and 0.94), BIAS (1.10, 1.42, and 2.31), the probability of detection (0.79, 0.78, and 0.67), false-alarm ratio (0.28, 0.45, and 0.73), and threat score (0.61, 0.47, and 0.25). Possible sources of error related to the validation procedure are presented and discussed. The validation showed that the proposed model (or neural network) can grab the physical content inside the dataset, and its performance is quite encouraging for the first and second hours to nowcast significant instability events in the study area.

Key words: neural networks; nowcasting; significant instability event.

Introduction

Aviation is negatively or positively influenced by the atmospheric conditions at any place and time (Ahrens, 2008). In particular, the Terminal Area (TA) of an airport is the area where the aircraft are waiting for landing or take-off and, thus, is quite sensitive to weather conditions. The air traffic controllers and pilots require precise information about the weather conditions at the TA to make short-term decisions that fall into the time scale of nowcasting, which ranges from the interval of a few minutes up to 6 h. During the few last decades, various works associated with nowcasting—for example, Wilson (1966), Wilk and Gray (1970) and others—have initially proposed nowcasting approaches based on extrapolations of radar data to generate nowcasting of thunderstorms. To follow up this idea, the convective tracking approaches were improved by including the cell evolution in time and intensity using radar data (Dixon and Wiener 1993). Wilson et al. (1998) presented a review of the nowcasting techniques developed during the 1960s and 1970s. The advancement of parallel computing and data availability allowed a numerical weather model to assimilate via rapid update cycle (and, more recently, via rapid refresh method) mesoscale data such as satellite and/or radar data to nowcast convective systems. Several authors have addressed the latter in the last two decades or so—e.g., Xue et al. (2003), Sun and Wilson (2003), Schroeder et at. (2006), Liu et al. (2008) and others. Mueller et al. (2003) proposed a sophisticated system to nowcast (up to 1 h) thunderstorm locations based on a combination of surface meteorological, radar, satellite data and numerical modelling, which considers the storm stages. Mass (2012) provided a comprehensive review of nowcasting including current developments and future challenges. Considering the aviation application, Isaac et al. (2006), Isaac et al. (2011) and Isaac et al. (2012) presented a sequence of works that resulted in a refined nowcasting system for aviation that uses data from numerical models, surface observations, radar, satellite and a microwave radiometer to generate nowcasts for principal airports in Canada up to approximately 6 h. In contrast, in Brazil, a meteorologist currently uses his experience to integrate different in situ meteorological observations and/or atmospheric model outputs using conceptual models on how the atmosphere works to generate nowcasts at principal airports. In particular, the TA of Rio de Janeiro, the focus of this study, has five airports (see Figure 1) whose flights are significantly affected (by delays and trajectory changes), especially during the approximations for landing or take-off, by Significant Instability Events (SIE), which are normally associated with convective weather. Groisman et al. (2005) presented evidence that the incidence of convective weather has increased approximately 58% per

year in south-eastern Brazil—where the Rio de Janeiro TA is located—since the 1940s. Therefore, the objective here is to present an Automated Nowcast Model (ANM) to generate short-term and local-specific predictions of SIEs, based on neural network techniques, for the fight TA of Rio de Janeiro, Brazil.

2. Meteorological datasets and study area

This study used four datasets from 1 January 2007 to 31 December 2008, as follows:

- TEMP is the meteorological code used to report profiles of atmospheric variables and is normally generated daily at 0000 UTC and 1200 UTC on all radiosonde stations, one of which, in this work, is located at Galeão´s Airport, whose international aviation code is SBGL, where SB and GL denote Brazil and Galeão, respectively (see Figure 1). The TEMP-coded dataset was obtained online from http://weather.uwyo.edu/upperair/sounding.html;
- METAR and SPECI are meteorological codes employed to report hourly surface meteorological conditions and significant change (decline or improvement) in the weather condition, at any time from the full hour. Figure 1 shows the locations of five surface meteorological stations (represented by red icons) in the Rio de Janeiro metropolitan area. The SPECI data were used only for the model validation. The stations (or airports) are Galeão (SBGL), Santa Cruz (SBSC), Santos Dumont (SBRJ), Jacarepaguá (SBJR), and Afonsos (SBAF). The data were obtained at the URL address mentioned above;
- rain rate (RR) is obtained from twenty-nine rain gauges (represented by yellow triangles in Figure 1) distributed over the Rio de Janeiro metropolitan area. The data were obtained from http://www.rio.rj.gov.br/alertario/ and collected by Alerta Rio's System, which belongs the City Hall of Rio de Janeiro; and
- lightning reports, regularly collected by the National Integrated Lightning Detection Network (RINDAT), characterize each occurrence by indicating location (latitude, longitude), intensity polarity (cloud to ground or ground to the cloud), and time (UTC with accuracy in milliseconds). ELETROBRAS FURNAS Company kindly made the data available.

Table 1 summarizes all information on the datasets used for ANM training, testing and validation in this study. Figure 1 shows the study region and the flight terminal area of Rio de Janeiro.

3

3. Methodology and algorithm description

Meteorologists have limited windows of time in which to integrate all available data and generate a nowcast, as stated by Mueller et al. (2003). Therefore, the idea is to create an automated nowcast model in which a neural network algorithm is used for data fusion, similar to the work performed by Cornman et al. (1998) for detecting and extrapolating weather fronts. At present, one may find applications of neural network in numerous fields of science, such as modelling, time series investigations, and image pattern recognition, owing to their capability to learn from input data (Haykin, 1999). Normally, stages of neural networks are denoted by a global function (Equation 1), as described by Bishop (2006)—for example:

$$y_k(x, w) = \sigma\left(\sum_{j=0}^{M} w_{kj}^{(2)} h\left(\sum_{i=0}^{D} w_{ji}^{(1)} x_i \right) \right)$$

(1)

where x_i and y_k are the input and output, respectively; (1), (2) and W_{ji}, W_{kj} represent the input layer, hidden layer and the connection weights (that should determinate) between input and hidden layers and hidden and output layers, respectively; D and M are the number of inputs and number of neurons in the internal layer, respectively; and σ and h are linear and no linear transfer functions between the neural network layers, respectively. Thus, determination of the output via Equation 1 crucially depends on the values of the weights that are worked out, similarly as in a multiple linear regression using a set of inputs and outputs; however, instead, to minimize the distance as in nonlinear regression, the neural networks attempt to minimize the cost function. Given that the SIE forecast problem requires a categorical output, it was decided to use probabilistic neural networks, initially proposed by Specht (1990, 1991), which is based on radial-basis function (RBF), A RBF network consists of three layers: the input layer; the second layer (or hidden), apply a non-linear transformation, denoted as h that, here, is Gaussian function, of the input space to the hidden space. The third layer, the outgoing, is linear (σ), providing the network response. Further details about neural networks and their applications may be found in Pasini et al. (2001), Haykin (1999), Pasero and Moniaci (2004), Bremnes and Michaelide (2005), Bishop (2006), Haupt et al. (2009) and Hsieh (2009).

Figure 3 depicts a general flowchart for the proposed automated nowcasting model. It has four major steps: (1) data processing; (2) definitions of input and output variables; (3) training and testing; and (4) validation. These steps are described below.

3.1 Step 1—Data processing:

All datasets were sorted chronologically, and their statistical consistency was observed, resulting in 63,320 h of meteorological records. Based on weather conditions reported by METAR, each meteorological record was classified into two classes—"0" and "1", representing nonexistence of important weather conditions (low impact to flight flow) and the existence of significant atmospheric instability (or SIE, as previously defined) for flights in the TA of Rio de Janeiro, respectively. Table 1 shows all weather conditions reported in terms of METAR code and their classification per class.

3.2 Step 2—Input and output definition:

ANM data fusion is based on a neural network, which must be sequentially trained, tested and subsequently validated to forecast the presence or absence of SIEs. The latter corresponds to the learning process of a neural network. The input and output variables play an important role in ANM data fusion and should be previously defined.

3.2.1 Input variables

These variables are the predictors of ANM and indicate the atmospheric stages of SIEs in the study area that are used by the ANM during its learning process. A meteorological record is composed of primary and derived variables that are extracted from METAR, TEMP, and RR and calculated using primary variables. The purpose of ANM is to nowcast SIEs and other weather conditions; therefore, all inputs (or predictors) should thermodynamically represent the presence or absence of SIE, which are embedded in the meteorological records utilized to train/test and validate the ANM. The latter should be able to classify or forecast weather conditions of classes numbered as "0" and "1", and its performance is evaluated by cross-validation with observations as presented later. The criterion to select input (primary and derived) variables is based on a conceptual model of how the atmosphere works—particularly during SIE occurrence, which have typical atmospheric patterns. Several input variables are used—for example,

atmospheric instability indices, i.e., K-index (K) = $(T_{850} - T_{500}) + Td_{850} - (T_{700} - Td_{500})$, where T_z and Td_z represent temperature and dew point, respectively, in Celsius degrees, and z is the given atmospheric pressure in hPa); Total Totals (TT) = $T_{850} + Td_{850} - 2T_{500}$; Lapse Rate (LR), represented by LR = $1000(T_{500} - T_{700})/ (GPH_{500} - GPH_{700})$, where GPH denotes the geopotential height; and others defined in columns three and four of Table 1. At the beginning, many inputs were generated. However, with regard to the neural network training, it is necessary to adopt a method to prune collinear inputs that bring no new information and, thus, could reduce the network performance. Pasini and Ameli (2003) have investigated heuristic pruning methods. Here, autocorrelation was selected and enforced to remove collinearity of the input. Twelve variables then remained, divided into eight primary and four derived variables as listed in columns three and four of Table 1, respectively.

3.2.2 Output variables

The output is defined as weather conditions reported in METAR codes and divided into two classes, "0" and "1", which represent the absence and presence of SIEs, respectively, as shown in Table 2. In other words, classes 0 and 1 indicate nonexistence of significant instability and existence of significant instability (i.e., weather condition of METAR code as T, TL, TRW-, TRW, TRW+) in the TA of Rio de Janeiro, respectively.

Following Pasini (2015) and aiming to avoid the overfitting problem during the learning process of the neural network, which is represented by step 3, the meteorological records were divided into three subsets: training, testing and validation. Figure 4 (a) shows the initial training and testing datasets representing 70% of the original records (or 44,324) with 30% (or 18,996) for validation, as shown in Figure 4 (b).

3.3 Step 3—Neural Network Training and Testing

The internal number of neurons (previously defined as **M**) of probabilistic neural networks is here determined based on cascade-correlation algorithm suggested by Fahman and Lebiere (1990). Figure 2 shows generally an example of a cascade forward network for five inputs and one output. The training and testing are performed in an iterative cycle composed of a looping of two phases, which are executed using a specific

6

dataset (initially the one in Figure 4 (a), which could be artificially modified until the optimal dataset is reached, as described in step 4), and a constant number of inputs (defined as **D** is equal to twelve). The two phases are described as follows:

i) It starts with a minimal (only one neuron) internal layer of the neural network (represented generally by Equation 1) and automatically adds new hidden neurons one at a time, in each round, finally resulting in a multilayer structure with the input connection frozen (represented by squares in Figure 2); and

ii) The follow-on neural network is applied to the test dataset, and the error is calculated. There are then two options: first, return to (i) if the test error has not increased from the previous round and the number of neurons in the internal layers is less than 150; or second, to go step 4, which means that the final (or that could be an optimum) neural network configuration (or ANM) has been obtained.

3.4 Step 4—Validation:

This step compares the SIE forecasts (output) of ANM with the true observations, which are assumed to have at least one of two conditions:

a) weather conditions (class 1 of Table 2) reported by METAR or SPECI (corresponding the validation dataset in Figure 4 (b)); and/or

b) lightning reported inside a 50-km radius centred at Galeão airport during a 1-h period. The lighting data are included in the validation because the weather conditions reported in METAR or SPECI represent an observation by the meteorologist at an instant of time; therefore, sometimes it does not correctly represent an entire one-hour period, which is the minimum time interval for an ANM forecast, and the lightning data will be continuously generated during the entire ANM forecast time and beyond the METAR observation, which depends on the meteorologist's observation skills. The lightning data allow the ANM forecast verification to be spread out to encompass the entire flight terminal area of Rio de Janeiro. Moreover, it is assumed in this work that the presence of lighting is related with SIE. Therefore, these two conditions will certainly permit a better ANM validation, which is accomplished via a two-dimensional contingency table. The calculation of five categorical statistics used to verify the frequency of correct and

incorrect forecasted values is performed as follows: 1) proportion correct (PC), which shows the frequency of the ANM forecasts that were correct (a perfect score equals one); 2) BIAS, which represents the ratio between the frequency of ANM estimated events and the frequency of ANM observed events (a perfect score equals one); 3) probability of detection (POD), which represents the probability of the occasions when the forecast event actually occurred (hits), and the scale varies from zero to one, where one indicates a perfect forecast; 4) false-alarm ratio (FAR), which indicates the fraction of ANM-predicted SIEs that did not occur (a perfect score equals zero); and 5) threat score (TS), which indicates how the ANM forecasts correspond to the observed SIEs (a perfect score equals one). In particular, the TS is relatively sensitive to the climatology of the studied event, tending to produce poorer scores for rare events, such as an SIE. Therefore, the model is considered to be optimal when it creates SIE nowcasting with scores as near perfect as possible for the five statistics described (Wilks, 2006).

Finally, if the validation results of the ANM do not indicate satisfactory performance, a normal procedure is to rearrange the representativeness of the target class one in the training data (i.e., modifying the training/testing dataset) and then go to step 3 and repeat step 4 in Figure 3. Otherwise, the optimal model is reached. The ANM training strategy and results are discussed in the next section.

4. Analysis and results

To assess the performance of the nowcasting system proposed for the TA of Rio de Janeiro, the ANM output variables were divided into two classes as previously defined—namely: class zero (no SIE) and class one (SIE). Figure 4 (a) and Figure 4 (b) depict the frequency of the classes in the initial (1st) training/testing and validation datasets, respectively, corresponding to 70% and 30% of the total number of meteorological records. It is observed in Figure 4 (a), that class frequencies are not proportionally distributed. In particular, class one (defined as SIE) is poorly represented, accounting for approximately two percent of all meteorological records. This increases the difficulty of the neural network learning process; for phenomenon knowledge, a better representation of target class one is needed in the training dataset—i.e., class one should have a higher weight than the other classes or at least a similar weight to another class in the training dataset—to facilitate better neural network training/testing. The following paragraphs summarize the strategy to overcome the low frequency of SIEs in

the sequence of preparation/testing executed in this work in the procedure to achieve the optimal model, as illustrated in Figure 3.

4.1 Neural network training

Neural network training is a time-consuming activity, and to overcome the mentioned problem, a common strategy is to alter the training dataset—for example, by taking the original data as a reference to artificially create another new training dataset by modifying the representation of the classes in the data population and testing the model performance to make an optimum and/or gradually reducing the input variables by evaluating a particular variable relevance (or contribution) for the output results. The latter was not performed in this work, and the input number was held constant and equal as previously explained in §3.2. In fact, there is no straightforward set of calculations to accomplish this goal. It is significant to observe that the validation dataset shown in Figure 4 (b) has similar class frequencies to the original dataset, shown in Figure 4 (a). The idea is to provide real scenarios of rare events during the validation process. Table 3 presents the training scheme (or strategy) and attempts to convey the concept of successive training used in the present work. The training strategy is based on decreasing records of class 0 and keeping class 1 fixed in each training/testing executed by following the steps in Figure 3. The optimal ANM was obtained in the nth training corresponding to the dataset in Figure 4 (c). The resulting validation statistics were achieved by two options: first, by considering items a); and second, by considering items a) and b) of §3.4. The latter item (item b)—lightning reported inside a 50-km radius centred at SBGL airport during a 1-h period—represents an SIE. Table 3 shows categorical statistical verifications of the optimal model results. The ANM forecast performance slowly declines from the first to the second hour and declines more rapidly from the second to the third hour. By including the lightning data in the validation, the ANM results were improved, as shown by the first $^{(L)}$, second $^{(L)}$, and third $^{(L)}$ hours (highlighted in grey in Table 3). The comparison between the two validation datasets (with and without lightning data) shows that BIAS, POD, and FAR values improved by 14%, 11%, and 12% (for the first, second, and third hours); 3%, 3%, and 6% (for the first, second, and third hours); and 13%, 13%, and 5% (for the first, second, and third hours), respectively. In particular, the BIAS values improved more than the other statistics because of the inclusion of the lightning data in the validation. In addition, although TS normally tends to produce poorer scores for rare events, its results have

9

also improved here with the inclusion of lightning data in the validation of optimal training as shown in Table 3, column thirteen.

The best ANM result corresponds to the first hour. The BIAS is the lowest, equal to 1.10 (which means that the results slightly overestimated the observations for the considered forecasts); even so, the readings for PC, POD, FAR, and TS are quite respectable, equal to 0.99, 0.79, 0.28, and 0.61, respectively. The effects of the ANM for the second hour are slightly less useful than those for the first hour forecast but are nonetheless satisfactory. However, the statistical values for the third hour forecast are poorer than those for the second hour. One cause of the ANM's overall performance degeneration is that a neural network is a statistical model rather than a physical one, which means that the physical aspects are not included. In summary, it is possible to state that an optimal ANM should be able to forecast SIEs in the study area for up to 2 h.

4.2. Possible sources of error in the ANM validation

The ANM optimal model output is considered a hit when it corresponds to event observations, if at least one of two weather conditions in §3.4 is satisfied. In particular, the weather condition reported in the METAR or SPECI is obtained from a human observer and may have some inconsistencies. The latter is common in meteorological observations; thus, consciousness of such matters is important when interpreting results from METAR at a specific time. The ANM results are slightly biased as previously presented for first hour forecast; therefore, in an attempt to explain that BIAS, the study pursued an investigation of possible sources of error in the meteorological observations used to verify the model forecasts. First of all, with regard to the learning process, the training dataset was composed only of meteorological records with a unique true association between their output (as class 1) and input variables (represented somehow in the thermodynamic atmospheric pattern during the development of an SIE from the METAR records). In other words, the training used only meteorological records whose output was characterized as a true SIE and none. However, in the validation dataset, there are many meteorological records in which such a unique association (one-to-one relationship between input and output) is not always true; i.e., some meteorological records have a typical thermodynamic pattern of SIE (input), but the weather condition (output) does not correspond to an SIE (or prevailing actual weather situation). These records were used in the present study to verify ANM forecasts and have consequently produced the results in Table 3. A possible reason for false alarms and consequently

10

biased ANM results is that hourly METAR records represent quasi-instantaneous meteorological observations (which take approximately 10 min to generate and may carry inconsistencies); therefore, the weather condition (output) may be affected by a certain amount of subjectivity on the part of the meteorologist (see discussion below). These results have provided plenty of evidence that the validation parameters (i.e., weather condition report just mentioned in the METAR or SPECI in Table 2) are not totally appropriate for ANM validation because the METAR or SPECI are quasi-instantaneous observations and thus do not cover the entire ANM forecast time. The lightning data permit the ANM forecast verification to be spread out to encompass the entire TA of Rio de Janeiro. The comparisons between ANM forecasts and lightning detection have improved all statistical values.

4.3 Case Study

To elucidate the foregoing discussion, this section shows the ANM results for an SIE that occurred from 1500 to 2300 (local time) on 18 March 2009. Figure 5 depicts a synoptic weather situation through an enhanced GOES-10 (channel 4) satellite image at 1800 (local time), in which a cloud (or cloud complex) is classified, by an automatic stretch process, as a convective cell (which could certainly be associated with an SIE) if its top temperature is lower than minus 30°C. The red box roughly represents the TA of Rio de Janeiro, which is influenced by SIEs (located approximately at the centre of the red box) and where a complex convective cloud (with cloud top temperature equal to minus 70°C) is clearly observed in the east. On this day, the K, TT, and LR index values, calculated from the SBGL atmospheric profile, were equal to 33.64, 44.97, and 5.5, respectively, indicating that a typical atmospheric instability pattern was dominating the area. Table 4 presents a comparison between ANM forecasts (column four) and the weather observations made by the meteorologist and registered in the METAR (columns two and three) for the considered period. From this result, it seems that the ANM overestimated the possibility of an SIE (compare columns three and four). However, the problem of verification of the output of the ANM is difficult because the meteorologist's observation does not always give a more appropriate weather condition (or a prevailing condition) for comparison; therefore, biased results may be obtained from the ANM. Lightning has been coincidently detected (column five) for all ANM forecasts of SIEs during the time of this particular case study, which indicates an unstable atmospheric pattern (meaning true SIE) in the flight area of the airport influenced by the event. In

11

summary, the ANM forecasts usually capture the signs of an atmospheric instability pattern

5. Conclusions

In Brazil, the numerical prediction models have presently demonstrated certain difficulties in attempting to forecast local or short-term heavy rain, strong wind, and turbulence events that are normally associated with SIE occurrences. Hence, this work demonstrates an automated nowcasting model for short-term and local-specific forecasting of SIEs based on a neural network technique for the flight terminal area of Rio de Janeiro. The main findings of this study are as follows:

a) the optimal ANM results of SIE forecasts for the first and second hours are encouraging because the categorical statistical values are quite acceptable. The proposed model has a very low computational cost, and it is possible to say that the ANM could alternatively forecast short-term strong atmospheric instability;

b) the third hour ANM forecast has the highest BIAS; perhaps the main reason for the ANM performance degeneration in time is that the neural network model is purely statistical rather than physical, and its use should therefore be limited to short-term nowcasting, possibly up to a 2-h timeframe;

c) there is visible evidence that the validation data contain a certain amount of uncertainty. A key consideration regarding the ANM results versus validation data and possible sources of error should be addressed; i.e., the use of METAR or SPECI weather conditions is affected by subjectivity on the part of the meteorologist and sometimes does not represent prevailing weather conditions. The results and case study showed that ANM forecasts might falsely be classified as hits;

d) the inclusion of lightning data in the validation significantly improved the ANM statistic results and also provided evidence that weather conditions discussed in the previous item are not totally appropriate for ANM validation; and

e) finally, the study may conclude that the optimal ANM developed here is clearly capable of predicting signs of a local atmospheric instability pattern in the TA of Rio de Janeiro.

Future studies are planned to include other data sources in the learning process, such as numerical models, meteorological satellites, RADAR, and/or SODAR wind profiles.

Acknowledgements

Reference

Ahrens, C. D.: Meteorology Today - Introduction to Weather Climate and Environment. 9th Edition, Brooks/Cole, CA, USA, 2008.

Bishop, C. M.: Pattern Recognition and Machine Learning, Springer, New York, NY, USA, 227–229, 2006.

Bremnes, J. B. and Michaelides, S. C.: Probabilistic visibility forecasting using neural networks, Pure Appl. Geophys., 164, 1365–1381, 2007.

Cornman, L. B., Goodrich, R. K., Morse, C. S., and Ecklund, W. L.: A fuzzy logic method for improved moment estimation from Doppler spectra, J. Atmos. Ocean. Tech., 15, 1287–1305, 1998.

Dixon, M.J. and Wiener, G.M.: TITAN: Thunderstorm identification, tracking, analysis, and nowcasting--a radar-based methodology. Journal of Atmospheric and Oceanic Technology, 10, 785-797, 1993.

Groisman, P. Y., Knight, R. W., Easterling, D. R., Karl, T. R., Hegerl, G. C., and Razuvaev, V. N.: Trends in intense precipitation in the climate record, J. Climate, 18, 1326–1350, 2005.

Haupt, S.E., Marzban, C., Pasini, A.: *Artificial Intelligence Methods in the Environmental Sciences*, Springer, 424 pp, 2009.

Hsieh, W. W.: *Machine Learning Methods in the Environmental Sciences: Neural Networks and kernels*. Cambridge university press, 2009.

Isaac, G. A., Bailey, M., Cober, S. G., Donaldson, N., Driedger, N., Glazer, A., Gultepe, I., Hudak, D., Korolev, A., Reid, J., Rodriguez, P., Strapp, J. W. and Fabry, F.: Airport Vicinity Icing and Snow Advisor. AIAA 44th Aerospace Sci. Meeting and Exhibit, Reno Nevada, AIAA-2006-1219, 2006.

Isaac, G. A., Bailey, M., Boudala, F., Cober, S.G, Crawford, R., Donaldson, N., Gultepe, I., Hansen, B., Heckman, I., Huang, L., Ling, A., Reid, J., Fournier, M.: Decision Making Regarding Aircraft De-Icing and In-Flight Icing Using the Canadian Airport Nowcasting System (CAN-Now). In SAE 2011 International Conference on Aircraft and Engine Icing and Ground Deicing 13-17 June 2011, Paper Number: 2011-38-0029; DOI: 10.4271/2011-38-0029.

Isaac, G.A., Bailey, M., Boudala, F.S., Cober, S.G., Crawford, R.W., Donaldson, N., Gultepe, I., Hansen, B., Heckman, I., Huang, L.X., Ling, A., Mailhot, J., Milbrandt, J.A., Reid, J. and Fournier, M.: The Canadian airport nowcasting system (CAN-Now). Accepted to Meteorological Applications, 2012.

Haykin, S.: Neural Networks: A Comprehensive Foundation, Prentice Hall New Jersey, New Jersey, USA, 1–24, 1999.

Liu, Y., Warner, T. T., Bowers, J. F., Carson, L. P., Chen, F., Clough, C. A., Christopher, A. D., Craig, H. E, C. h., Halvorson, S. F., Terrence, W. H. Jr., Lachapelle, L., Malone, R. E., Daran, L. R., Sheu, R-S., Swerdlin, S. P. and Weingarten, D.S.: The operational mesogamma-scale analysis and forecast system of the US Army Test and Evaluation Command. Part I: Overview of the modeling system, the forecast products, and how the products are used. *Journal of Applied Meteorology and Climatology*, *47*(4), 1077-1092, 2008.

Mass, C.: Nowcasting the promise of new technologies of communication, modelling, and observation. B. Am. Meteorol. Soc., 93(6): 797-809, 2012.

Mueller, C., Saxen, T., Roberts, R., Wilson, J., Betancourt, T., Dettling, S., Oien, N., and Yee, J.:
NCAR auto-nowcast system, Weather Forecast., 18, 545–561, 2003

Pasero, E. and Moniaci, W.: Artificial neural networks for meteorological nowcast, in: Computational Intelligence for Measurement Systems and Applications, CIMSA, IEEE International Conference on, Boston, MA, USA, 14–16 July 2004, IEEE, 36–39, 2004.

Pasini, A., 2015: Artificial neural networks for small dataset analysis. J Thorac Dis., 7(5): 953–960, 2015. doi: 10.3978/j.issn.2072-1439.2015.04.61

Pasini, A., Pelino, V., and Potestà, S.: A neural network model for visibility nowcasting from surface observations: Results and sensitivity to physical input variables, J. Geophys. Res. Atmos., 106, 14951–14959, 2001.

Pasini, A. and Ameli, F.: Radon short range forecasting through time series preprocessing and neural network modeling. Geophys. Res. Letters, 30, 2003. doi: 10.1029/2002GL016726.

Schroeder, A., Stauffer, D. R., Seaman, N. L., Deng, Gibbs, A., Hunter, G. K. and Young, G. S.: An automated high-resolution, rapidly relocatable meteorological nowcasting and prediction system. Mon. Wea. Rev., 134, 1237–1265, 2006.

Specht, D. F.: Probabilistic neural networks. In: IEEE T. Neural Networks, 3, 109–118, 1990.

Specht, D. F.: The general regression neural network. In: IEEE T. Neural Networks, 2(6): 568– 576, 1991.

Sun J., and J. W. Wilson.: The assimilation of radar data for weather prediction. Radar and atmospheric science: a collection of essays in honor of David Atlas, R. Wakimoto and R. Srivastava (Editors), Amer. Meteor. Soc., 175-198, 2003.

Xue, M., Wang, D., Gao, J., Brewster, K. and Droegemeier, K. K.: The Advanced Regional Prediction System (ARPS), storm-scale numerical weather prediction and data assimilation. Meteor. Atmos. Phys., 82(1), 139-170, 2003.

Wilk, K. E. and Gray, K. C.: Processing and analysis techniques used with the NSSL weather radar system. In *Preprints, 14th Conf. on Radar Meteorology, Tucson, AZ, Amer. Meteor. Soc* (pp. 369-374), 1970.

Wilks, D. S.: Statistical Methods in the Atmospheric Sciences: An Introduction, vol. 59 of International Geophysics Series, Academic Press, London, UK, 255–269, 2006.

Wilson, J. W.: Movement and predictability of radar echos. Tech. Memo, ERTM-NSSl-28, National Severe Storms Laboratory, 30 pp, 1966.

Wilson, J. W., Crook, N. A., Mueller, C. K., Sun, J and Dixon, M.: Nowcasting thunderstorms: A status report. *Bull. Amer. Meteor. Soc.*, *79*(10), 2079-2099, 1998.

Table 1 - Datasets and meteorological variables used in the distinct stages of development of the neural network-based automated nowcasting model. It covers a period from 1 January of 2007 to 31 December 2009.

Time series	Frequency and data period	Input: Primary variables Total number: 8	Input: Derived variables Total number: 4	Data percentage used for SNM training	Data percentage used for SNM validation	Validation variables	Output variable
		Predictors purpose: characterization of atmospheric conditions					
METAR (data are from SBGL, SBSC, SBJR, SBAF and SBRJ)	Hourly from 1 January 1997 to 31 December 2008	Dew point at surface	Julian day	70%	30%	Class 1 as in Table 2	Yes= class 1) or No= class 0)
TEMP (data are from SBGL)	Daily at 0000 and 1200 UTC from 1 January 1997 to 31 December 2008	Humidity at 850 and 500 hPa Pression at 1000, 850, 700, and 500 hPa	K, Vapour pressure at 1000, and 850 hPa ,			-----	
Rain rate (RR) per hour (data are from the 29 rain gauges)	Every 15 minutes from 1 January 1997 to 31 December 2008	RR for 1 hour	-----			-----	
Lightning[1] inside a radius of 50 km centred at SBGL	Varies	-----	-----	-----	100	1 (lightning) or 0 (no lightning)	

Table 2 – Weather condition classification in METAR and attributed ANM classes.

Class	METAR code	Weather condition	Class	METAR code	Weather condition
0	H	Haze	0	R	Moderate rain
	K	Smog		RF	Moderate rain with fog
	F	Fog		R+	Heavy rain
	L-	Light drizzle		R+ F	Heavy rain with fog
	L- F	Light drizzle with fog		RW	Showers
	L	Moderate drizzle		RW+	Heavy showers
	LF	Moderate drizzle with fog	1	T	Thunderstorms
	L	Heavy drizzle		TL	Thunderstorms with light drizzle
	R-	Light rain		TRW-	Thunderstorms with showers
	R- H	Light rain with haze		TRW	Thunderstorms with moderate showers
	R- F	Light rain with fog		TRW+	Thunderstorms with heavy showers

Table 3 – Strategy condition and final validation statistics of the optimal ANM. The ANM output equal to class one represents a true SIE (or yes) and class zero represents a false SIE (or no) forecast. The statistic values associated with the first [L], second [L], and third [L] are hours in which the ANM validation using the lightning data was included.

Training Strategy			Output class	Validation data	Neural network configuration (Number of hidden neurons)	Statistics for SIE and no SIE					
Training (from 1st to nth)	Training dataset and strategy	Number of Inputs				Hour	PC	BIAS	POD	FAR	TS
nth Optimum training	Gradually modifies for each looping in Figure 3 by decreasing classes 0 and keeping class 1 fixed	12	Yes or No (Yes= class 1) or (No= class 0)	Yes or No means classes one (including lighting existence in the period of 1 h) or zero in Table 2, respectively	123	1st	0.98	1,28	0.76	0.41	0.50
						1st (L)	0.99	1.10	0.79	0.28	0.61
					138	2nd	0.97	1.59	0.75	0.52	0.41
						2nd (L)	0.97	1.42	0.78	0.45	0.47
					134	3rd	0.94	2.64	0.61	0.77	0.20
						3rd(L)	0.94	2.31	0.67	0.73	0.25

19

Table 4 - ANM forecasts versus meteorological observations on March 18, 2009.

Local time	Weather condition (METAR)	Observed class	SNM class forecasts	Lightning detection
15	H	0	0	no
16	TRW-	1	1	yes
17	R	0	1	yes
18	R-	0	1	yes
19	H	0	1	yes
20	TRW-	1	1	yes
21	R+	0	1	yes
22	T	1	1	yes
23	TRW+	1	1	yes

Figure 1 - Satellite image of Rio de Janeiro´s metropolitan area. Yellow triangles [red squares] indicate location of the twenty-nine rain gauges from Alerta Rio's System that belongs the City Hall of Rio de Janeiro [five airport meteorological stations]. Source: Adapted from www.google.com.br/maps.
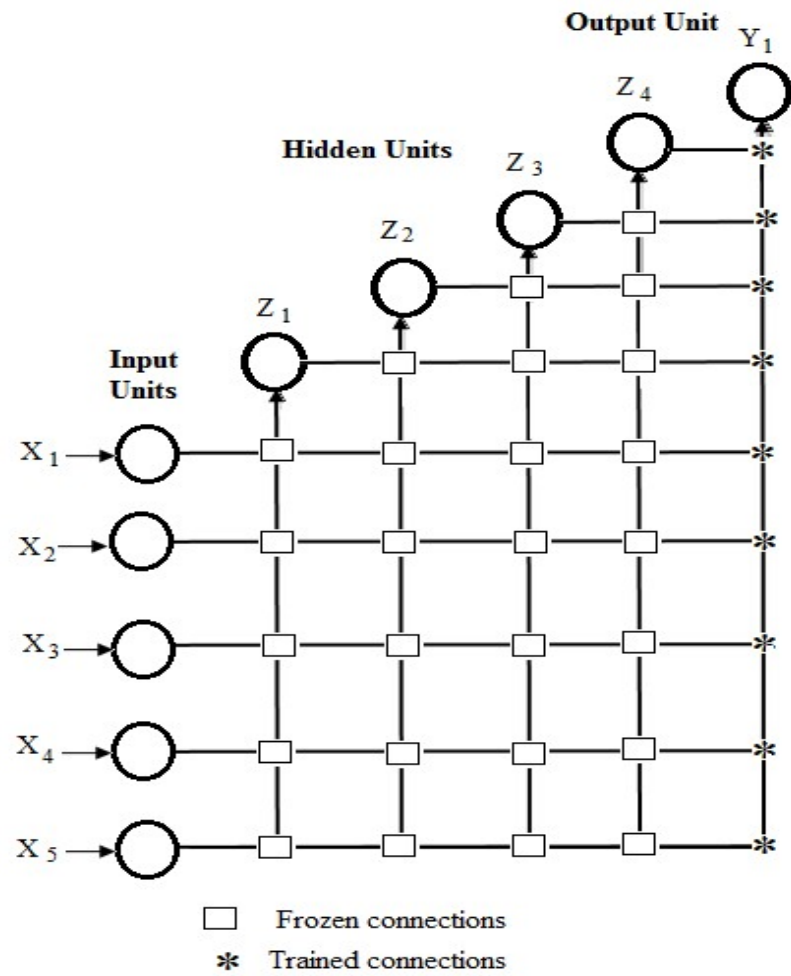
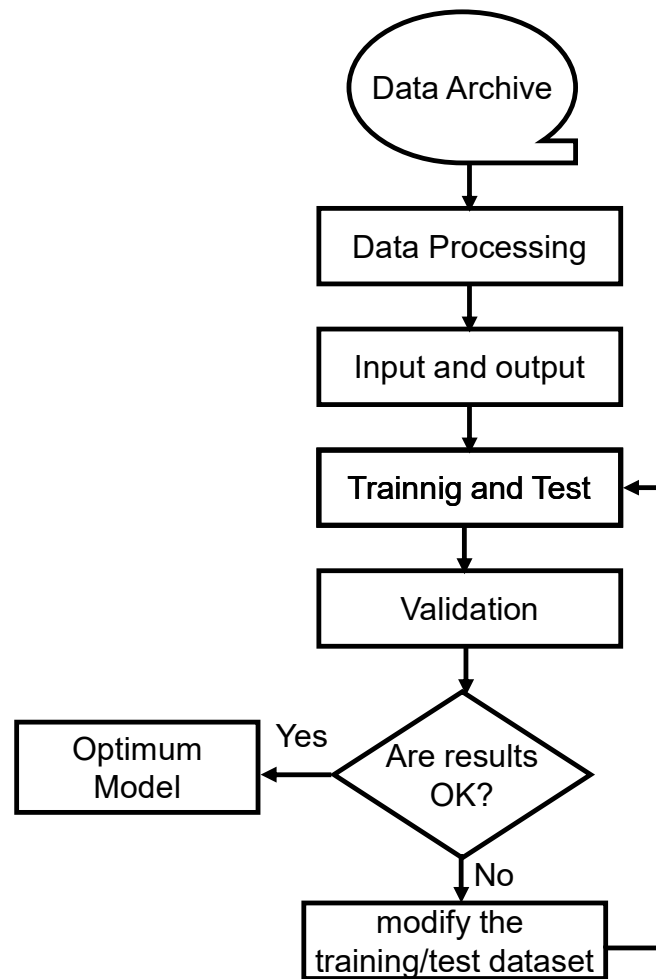Figure 2 - A schematic view of a cascade forward network with five inputs.

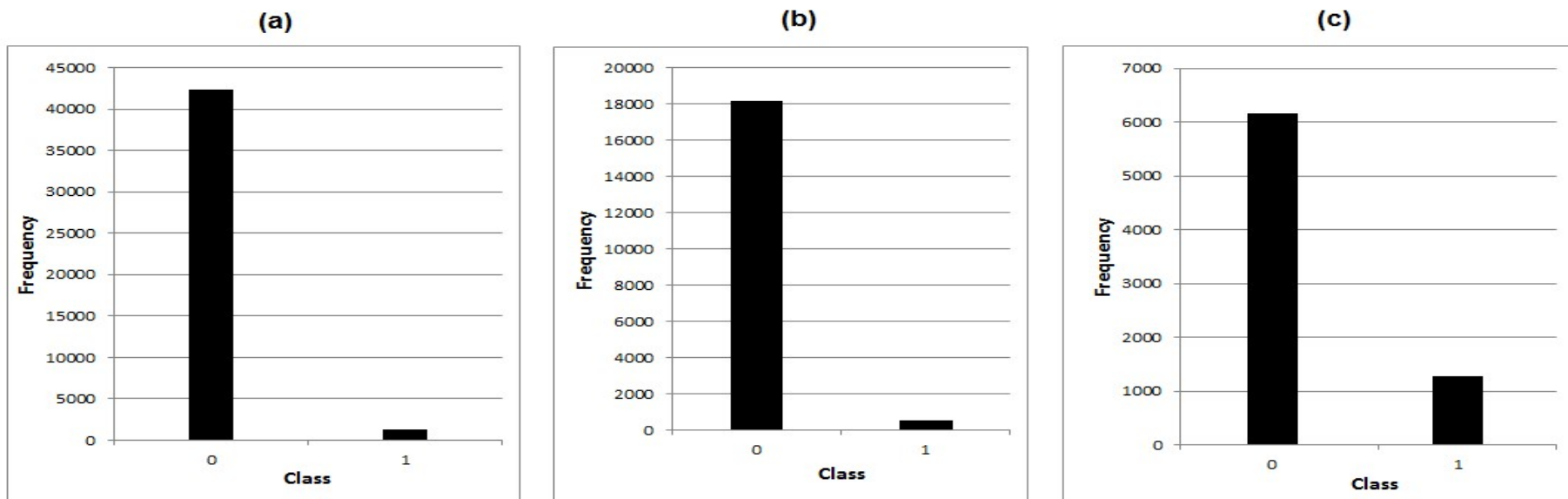Figure 3 - Automated Nowcast Model flowchart.

 Figure 4 – Histograms of frequency accordingly to two classes "0" and "1" that represent no SIE and SIE, respectively: (a) and (b) show initial class distribution of training/testing and validation datasets that correspond to 70% (or 44,324) and 30% (or 18.996) of meteorological records, respectively. (c) similarly presents class distribution of meteorological recordings for optimal training.
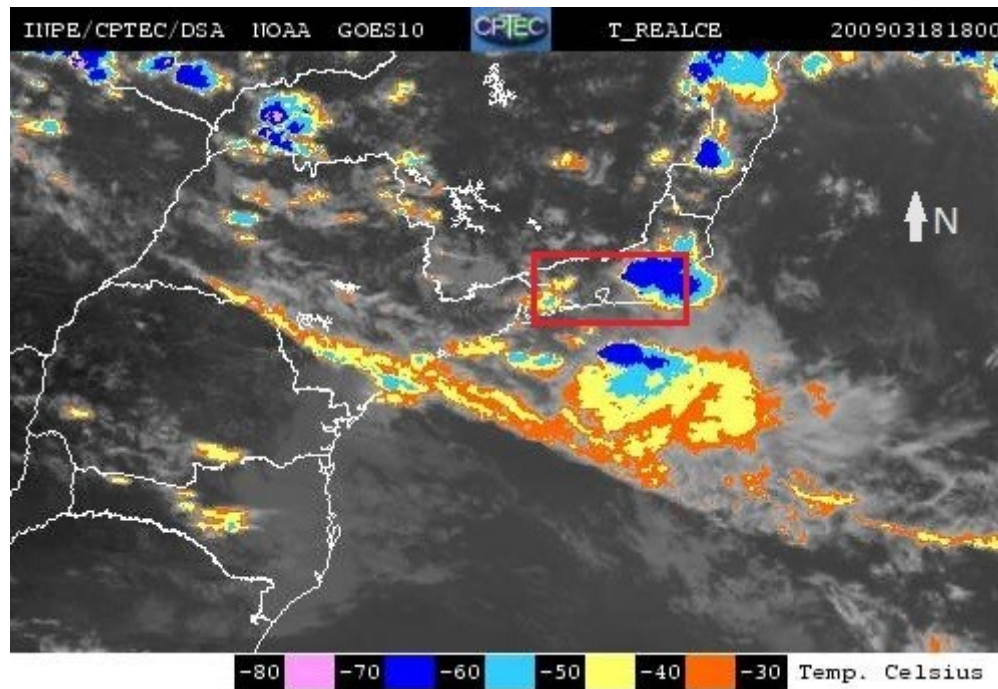
Figure 5- GOES-10 (channel 4) extracted and adapted from www.cptec.inpe.br that represents the synoptic weather situation at 1800 (local time) on 18 March 2009, where the top convective cloud temperatures are categorized by a temperature range from -30°C to -80°C. The red box roughly represents the study region.